I&EC research
Industrial & Engineering Chemistry Research

Article

pubs.acs.org/IECR

Entrainment Performance and Model of Multidowncomer Sieve Trays

Rui Cao,[†,‡,§] Yu He,[†] Huaming Guo,[*,‡] and Yansheng Liu[*,†]

[†]State Key Laboratory of Heavy Oil Processing, China University of Petroleum, Beijing 102249, People's Republic of China
[‡]School of Water Resources and Environment, China University of Geosciences (Beijing), Beijing 100083, People's Republic of China

ABSTRACT: The experiments about entrainment performance, as well as mass-transfer efficiency, of multidowncomer (MD) sieve tray were investigated in a 1200-mm-diameter tower with air/water system. The results indicate that the entrainment rate of MD sieve tray is lower and its behavior with increased liquid rate contradicts that of the conventional sieve tray. According to the nonmonotone variation phenomenon of entrainment at various liquid loads given by Lu and Kister, we developed the Double-Transition Point Theory to interpret the entrainment features under different contact regimes and the entrainment mechanism of MD sieve tray. By comparing the correspondence match of entrainment, pressure drop, and efficiency curves, we discussed the operating upper limit and mass-transfer efficiency. Therefore, based on the formulas of Fell's and Hunt's correlations, we developed the model for MD sieve tray where a semitheoretical derivation on entrained droplets in the froth regime was made.

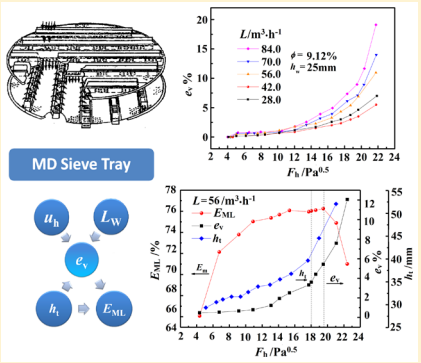

1. INTRODUCTION

The multidowncomer (MD) sieve tray is a type of high-flux tray aiming to boost liquid capacity. A detailed introduction about the MD sieve tray has been reported in a previous study of this work.[1] Particularly, there are several rectangular-truncated downcomers suspended from the MD tray. The weir length of the MD tray is 2−5 times longer than the conventional sieve tray, which makes the liquid weir load decrease significantly. There is no seal pan on the MD tray, thus allowing more vapor capacity for a larger bubbling area. Delnicki et al.[2] indicated that the MD sieve tray can operate fine at >122 $m^3\ m^{-1}\ h^{-1}$ for the distillation tower, and even up to 200 $m^3\ m^{-1}\ h^{-1}$ for the water scrubber. It is especially applicable for the operations at a high liquid rate (L) or high ratio of liquid rate to gas rate (L/V), such as in ethylene and p-xylene distillation towers.

The MD sieve tray has been widely used in industry. Universal Oil Products Co. (UOP) had purchased MD technologies from Union Carbide Co. (UCC) and then applied for several patents, such as the Enhanced Efficiency Multi-Downcomer (EEMD) tray and the Enhanced Capacity Multi-Downcomer (ECMD) tray. It was reported that the throughput of a demethanizer was improved by at least 30%, where the four-pass sieve tray was replaced by a MD tray.[3] In addition, Nutter and UOP combined a multidowncomer with a Nutter V-Grid fixed valve into a VGMD tray,[4] which provided better performance than the conventional sieve tray.

In China, the MD sieve tray was employed initially in a water scrubber and a carbonation tower[5] for ammonia synthesis, as well as evaporation tower and condensation tower. Its applications then were extended to the ethylene tower[6−8] and aromatics distillation processes.[9] At present, it has been gradually promoted to the fields of refineries, petrochemicals, fertilizers, fine chemicals, the pharmacy industry, and so on. Some modifications of MD technologies, such as DJ tray,[10−13] were developed, and the computational fluid dynamics (CFD) simulations[14] for the hydraulic characteristics of MD tray have received much attention.

There are many studies on entrainment and some achievements were made. Kunesh et al.,[15] Kister et al.,[16,17] and Van Sinderen et al.[18] provided an overview of the discussion on tray behavior. They noted that, at higher vapor velocities, ascending vapor lifts and carries over much of the tray liquid, causing the tower to flood. Excessive entrainment can cause an incorrect efficiency estimate and unsuitable hydraulic prediction correlations would lead to high capacity expectations. Locket et al.[19] and Jaćimović[20] gave an analytical solution for liquid plug flow on the tray and obtained a numerical solution for partially mixed liquid, from which the effect of entrainment on tray efficiency can be determined for all conditions. On the basis of the exploration for a gas/liquid regime, Kister et al.[21−23] and Lu et al.[24] made a deep study on the entrainment-formation mechanism. Hunt et al.,[25] Fell and Kister et al.[21−23] proposed the entrainment correlations in various regimes. Bennett et al.[26] developed a phenomenologically based model for froth height using the assumption of both vapor- and liquid-continuous zones within the total froth height. The model demonstrates the importance of liquid and vapor rates and determines that the Weber number (We) (and, therefore,

Received: February 18, 2017
Revised: May 16, 2017
Accepted: May 18, 2017
Published: May 18, 2017

DOI: 10.1021/acs.iecr.7b00702
Ind. Eng. Chem. Res. 2017, 56, 6755−6763

Table 1. Summary of Entrainment Correlations on Sieve Tray

author	entrainment correlations
Hunt et al.[25]	$e_v = 7.75 \times 10^{-5}\left(\frac{73 \times 10^{-3}}{\sigma}\right)\left(\frac{u_s}{T_s - h_f}\right)^{3.2}$
Kister et al.[21,22]	$e_{v,froth} = 3.51 \times 10^{-3}\left(\frac{u_s}{T_s - h_f}\right)^2 d_h^{0.5}(1 + \zeta)$
	$e_{v,spray} \propto \left(\frac{\rho_G u_s^3}{\rho_L L_w g}\right)^{1.17}\left(\frac{u_s \rho_L \mu_G}{\rho_G \sigma}\right)^{1.17}\left(\frac{h_{cl}}{(d_h T_s)^{0.5}}\right)^{4.68}$
Fell et al.[27] (air/water)	$e_v = K_1\left[\frac{u_s}{L_w^{0.25}}\frac{1}{(1 + K_2 h_w)}\frac{h_{cl}}{(d_h T_s)^{0.5}}\right]^{4.68}\left(\frac{\mu_G}{\sigma}\right)^{1.17}$
	mixed-froth regime: $K_1 = 20.5$, $K_2 = 2.62$; froth regime: $K_1 = 13.1$, $K_2 = 0$
	$e_{v,froth} = 0.00164\left(\frac{K_s^2}{g\phi_e T_s}\right)^{1.86}\left\{\frac{g h_{cl}}{K_s^2} + \frac{9\sqrt{3}}{2\phi}\left[1 + 6.9\left(\frac{d_h}{h_{cl}}\right)^{1.85}\right]\right\}^{1.86}\left(\frac{\rho_L}{\rho_G}\right)^{0.5}$
	$e_{v,spray} = 0.0050\left(\frac{K_s^2}{g\phi_e T_s}\right)^{1.26}\left\{\frac{g h_{cl}}{K_s^2} + \frac{9\sqrt{3}}{2\phi}\left[1 + 4.77\left(\frac{d_h}{h_{cl}}\right)^{3.29}\right]\right\}^{1.26}\varepsilon^{\beta}\left(\frac{\rho_L}{\rho_G}\right)^{0.5}$
	$K_s = u_s\sqrt{\frac{\rho_G}{\rho_L}},\ h_{cl} = \phi_e h_{fe},\ h_{fe} = h_w + C\left(\frac{L_w}{\phi_e}\right)^{2/3}$
Bennett et al.[26] (air/water)	$C = 0.501 + 0.439\exp(-137.8h_w),\ \phi_e = \exp(-12.55K_s^{0.91})\varepsilon = \frac{h_{cl}}{h_f}$
	$\beta = 0.5\left\{1 - \tanh\left[1.3\ln\left(\frac{h_{cl}}{d_h}\right) - 0.15\right]\right\}$
	$h_f = 1 + \left[1 + c\left(\frac{h_{cl}}{d_h}\right)^d\right]\left(\frac{Fr}{2}\right)$
	froth: $c = 4.77$, $d = -3.29$; spray: $c = 6.9$, $d = -1.85$
	$Fr = \left(\frac{u_{d0}^2}{g h_{fe}}\right),\ u_{d0} = 3K_s\sqrt{\frac{\sqrt{3}}{\phi\phi_e}}$

droplet size and surface tension) has little effect on froth height. Moreover, Lockett[27] made an overall description in a review of entrainment characteristics and correlations. In 2012, Uys et al.[28] described the froth behavior of the sieve tray and compared the entrainment data with existing correlations. In 2015 and 2017, they carried out the experiments on how the gas/liquid physical properties impacted the entrainment performance.[29,30] All the correlations mentioned above are listed in Table 1.

The above-mentioned studies mainly focus on the conventional sieve tray rather than MD. Until now, we have been forced to adopt the entrainment correlations of the conventional sieve tray for a MD sieve tray, which should be used with caution. Since the loading capacity of liquid phase on MD tray is greater than the conventional tray, two phases on MD are usually in the froth- or mixed-froth flow regime and splashing does not easily form. Therefore, the quantity of entrainment is much lower and its entrainment formation mechanism is different from conventional sieve tray. It means an entrainment value for MD tray predicted by the conventional sieve tray model is not reliable.

Furthermore, we cannot make direct appraisals of entrainment in industry, so we carried out the hydraulic and efficiency experiments of MD sieve tray in a 1200-mm-diameter tower and analyzed its entrainment performances. The experimental tower is of equivalent scale with industrial devices, which makes the data more reasonable. In addition, note that, in the early report of this work, the experimental data of tray pressure drop for the MD sieve tray has been validated by the industrial data of the ethylene distillation tower of Beijing Yanshan Petrochemical Company.[1] It shows that the experimental data agree well with the industrial data. Therefore, on the basis of the experimental data, we analyzed the entrainment mechanism and developed a new model for the MD sieve tray.

2. EXPERIMENTAL DEVICES

In this work, a 1200-mm-diameter tower with industrial scale was employed. Figure 1 shows the diagram of hydraulic experimental setup, where labels "7", "8", and "9" denote the experimental MD sieve trays (see Figure 2 and Table 2) and labels "4" and "5" represent the demister and the entrainment collecting device (see Figure 3), respectively. Others can be seen in the report of a previous study.[1]

DOI: 10.1021/acs.iecr.7b00702
Ind. Eng. Chem. Res. 2017, 56, 6755−6763

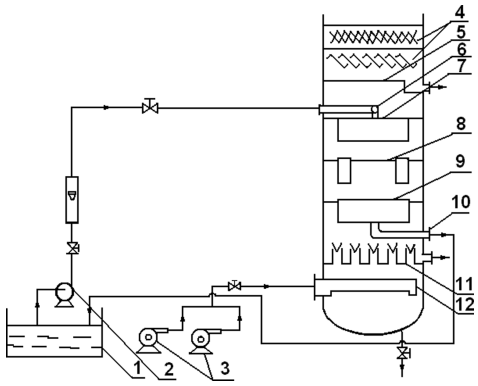

Figure 1. Diagram of the experimental setup. Legend: 1, water tank; 2, pump; 3, roots blower; 4, demister; 5, entrainment collecting device; 6, liquid distributor; 7, top experimental tray; 8, middle experimental tray; 9, bottom experimental tray; 10, water outlet; 11, weeping collecting device; and 12, gas distributor.

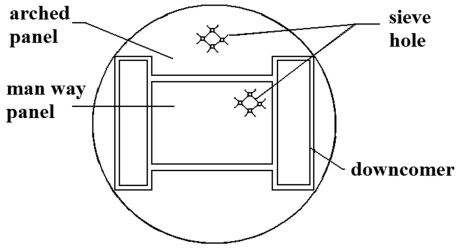

Figure 2. Schematic diagram of the MD sieve tray.

Table 2. Structure Dimensions of MD Sieve Tray

structure parameter	value
tower diameter	1.2 m
hole diameter	0.012 m
weir length	2.8 m
weir height	0.025 m
hole area	9.12%
downcomer spacing	0.8 m
downcomer length	0.6 m
downcomer width	0.1 m
downcomer numbers	2
tray spacing	0.4 m

In Figure 1, air is fed into the gas distribution pipe (12) by the root's blowers (3), the weep measurement system (11), the experimental tray (9, 8, 7), the entrainment measurement system (5, 4), and finally blown into the atmosphere. Water is pumped into the liquid distribution pipe (6) from water tank (1), which passes through the experimental tray (7, 8, 9) and finally returns to the water tank (1).

The entrainment collecting device (see Figure 3) is a single-pass sieve tray with a mesh and baffle demister, whose open area (9.12%) and hole diameter (12 mm) are the same as the experimental tray. When gas flows through two adjacent liquid-trap fins, the droplets trapped by the folding structure of the catches are led to the liquid sump along one side of the fin. Then, the finer mist is further captured by the mesh demister. Finally, the entrainment liquid is collected from the catches and sent to be measured.

On the other hand, tray efficiency was measured using an oxygen desorption method. A packed tower of oxygen absorption (see Figure 4) is introduced in our mass-transfer

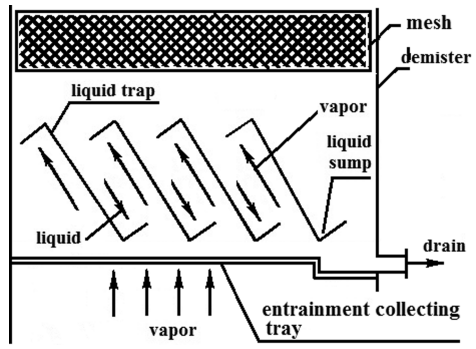

Figure 3. Diagram of the entrainment collection device.

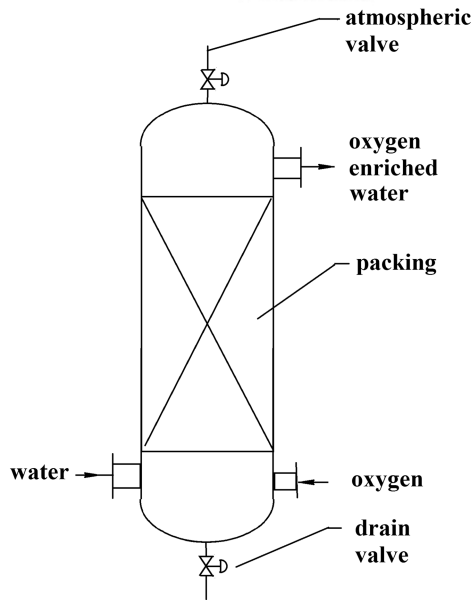

Figure 4. Oxygen absorption tower.

experiment for preparing oxygen-enriched water, while the above-mentioned experimental tower is used for oxygen desorption. Measuring the oxygen concentrations of water at inlet and outlet and substituting them into eq 1, we can obtain the Murphree liquid-phase tray efficiency (E_{ML}).[31]

$$E_{ML}\ (\%) = \frac{X_{in} - X_{out}}{X_{in} - X_{out}^{*}} \times 100 \quad (1)$$

The liquid sample point is shown in Figure 5, and the oxygen concentration of water is measured by a portable dissolved oxygen meter (Instrument, Model JPB-607).

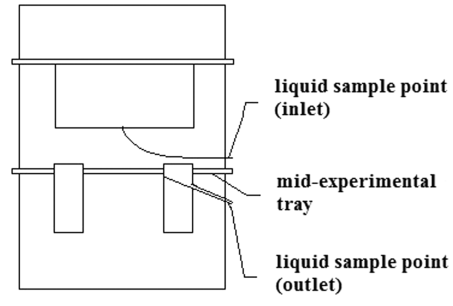

Figure 5. Schematic diagram of liquid sample point (tray efficiency).

DOI: 10.1021/acs.iecr.7b00702
Ind. Eng. Chem. Res. 2017, 56, 6755−6763

3. RESULTS AND ANALYSIS

3.1. Entrainment Data of MD Sieve Tray. In this work, the entrainment (e_v) data of the MD sieve tray at various hole kinetic energy factor, F_h ($F_h = u_h\sqrt{\rho_G}$) are summarized in Figure 6 and that under different liquid load (L) are summarized in Figure 7.

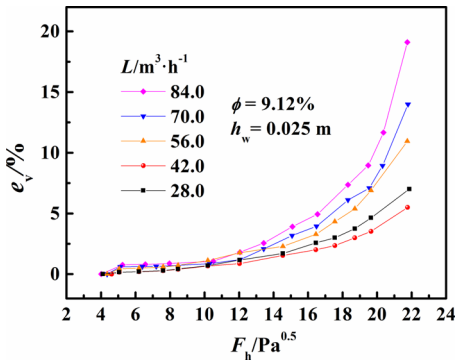

Figure 6. Effect of F_h on entrainment of the MD sieve tray.

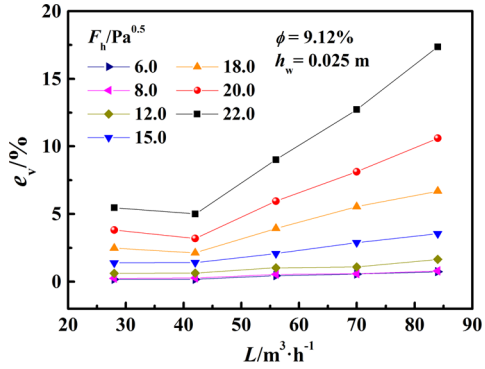

Figure 7. Effect of L on entrainment of MD sieve tray.

From Figure 6, we find that the e_v of the MD tray increases with increased F_h at a constant L, which is similar to that of the conventional sieve tray. When the gas velocity is low, e_v is slight, because the liquid layer is so heavy in the froth regime that it blocks the entrainment and makes some droplets join together. When the gas velocity is high, e_v increases rapidly, because of the gas/liquid contact status transfer from a froth regime to a mixed-froth regime, and liquid is more easily to break up into droplets under stronger shearing force.

Nevertheless, as shown in Figure 7, the entrainment variation behavior of MD sieve tray is significantly different from that of the conventional one with increased L: When gas velocity is at a constant, e_v decreases slightly at first and then increases rapidly. The higher the gas velocity, the more obvious the transition of e_v curve appears. However, the entrainment of the conventional sieve tray usually decreases with increased L.

3.2. Double-Transition Point Theory and Entrainment Mechanism of the MD Sieve Tray. The entrainment of MD sieve tray is relatively lower and its behavior under increased liquid load contrasts with the conventional one. This observation means that their entrainment mechanisms are different from each other.

In the early report, Lu et al.[24] has given the entrainment experimental data within a wide range for conventional tray (see Figure 8). It can be seen that the entrainment data is

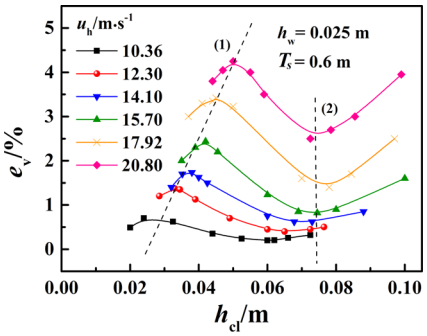

Figure 8. Effect of h_{cl} on entrainment (Double-Transition Point Theory). Note that the dotted line labeled as "(1)" is the first transition point line; the dotted line labeled "(2)" denotes the second transition point line.

nonmonotone—that is, e_v increases with L at first, and then goes down—and has a tendency to rise at last. Meanwhile, Kister et al.[21−23] commented that tray hydraulic characteristics are greatly dependent on two-phase flow regimes. Generally, the entrainment mechanism in the three major flow regimes varies as follows:

Froth regime: When the gas velocity is low and the liquid rate is high, gas can be transported through the liquid layer via the formation of bubbles under buoyancy. The airflow, in a fluctuating turbulent field with a high h_{cl}, cannot penetrate the liquid layer directly so there is almost no jet or spray in sight and effuse stably with some entrainment carried.

Mixed-froth regime: The loads of gas/liquid are both high, and the airflow is occasionally cut off because of the liquid bridge so that it cannot pass through the froth layer continuously. It is just a transition between the spray regime and the froth regime, where bubbling and jet exist simultaneously.

Spray regime: When gas velocity is high, yet liquid depth is low, liquid phrase is draw up into inverted hollow cones by pulsating gas jets, where the liquid sheets around the hole break up into small droplets to disperse into the gas phase. The droplets are entrained more intensely in the spray regime than in any other regime.

On the basis of these experimental data and phenomenon, it is believed that there are two transition points in the e_v−h_{cl} curves under constant gas velocity of hole (u_h).

When L is smaller, in the mean time (h_{cl}) is low. It is easier for gas to erupt through the liquid layer. Increased liquid load tends to boost the amount of entrainment due to more droplets. Whereas, after that, more liquid load would make the gas/liquid phase transform into the mixed-froth regime. In particular, it is more likely for more droplets to converge into bigger ones, which would form a liquid bridge and prevent other droplets from moving up. Therefore, it results in a decreased entrainment e_v with increased L. Then the first transition points emerge and can be illustrated as the dashed line labeled as "(1)" in Figure 8, which can be interpreted by the nonmonotone variation phenomenon of entrainment at various liquid loads given by Lu et al.[24]

Afterward, if L increases unceasingly, the layer of froth would grow thicker and thicker and the disengaging space, T_s-h_{fe}, would diminish gradually, where the mixed-froth regime is likely to transform to the froth regime. Consequently, the droplets are entrained more easily so that the e_v rises rapidly.

DOI: 10.1021/acs.iecr.7b00702
Ind. Eng. Chem. Res. 2017, 56, 6755−6763

The second transition points were illustrated as the dashed line labeled as "(2)" in Figure 8.

Apparently, the entire operating range can be divided into three parts by the two transition point lines. The spray region is on the left of dashed line (1), the mixed-froth region is between dashed lines (1) and (2), while the froth region is on the right of dashed line (2). In all, we call this rule of entrainment "Double-Transition Point Theory".

Generally, for the conventional sieve tray, it is easy to spray at high gas velocity, because of the shorter weir length. With increased L, the spray regime appears to transform to the mixed-froth one, where the resistance and capture of the liquid bridge play the dominating role in entrainment formation. Thus, the e_v behavior of the conventional sieve tray agrees with the decreasing part of the curves after the first transition point.

In contrast, the allowable liquid load of the MD sieve tray is higher than that of the conventional one, as is the height of the dispersion layer (h_{fe}), because its weir length is 2−5 times longer than that of the conventional one. The increased L makes the mixed-froth regime on the tray transform to the froth regime. Obviously, h_{fe} is the dominant factor of the MD tray. Moreover, the lower tray spacing (T_s) of the MD sieve tray also magnifies the influence of h_{fe}. For these reasons, the entrainment curve of the MD sieve tray seems to increase with increased L, just as the increasing part of the curves after the second transition point.

In addition, the MD sieve tray is mainly in the froth- or mixed-froth regime and usually operates with a lower entrainment.

3.3. Comparisons among Entrainment, Pressure Drop, and Efficiency of MD Sieve Tray. It cannot be ignored that the amount of entrainment is closely related to the surface of the droplets. The higher the gas velocity, the smaller the size of the droplets; hence, more fine droplets lead to more entrainment. Meanwhile, the residual pressure drop is defined as the excess pressure drop required to overcome surface tension when bubbles form at the orifice. It is obvious that the higher the gas velocity, the higher the residual pressure drop for surface energy. Figure 9 compares the entrainment and the

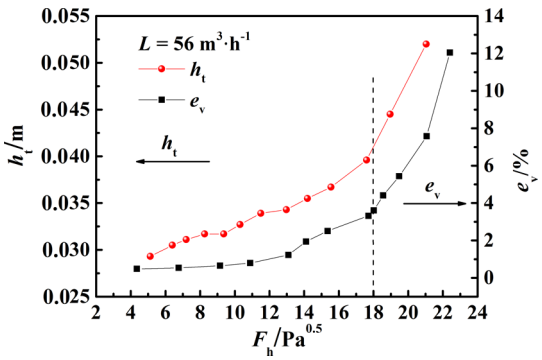

Figure 9. Comparison between entrainment and pressure drop of the MD sieve tray.

pressure drop curve of the MD sieve tray at 56 m^3 h^{-1}, where the left ordinate is the pressure drop of the tray (h_t), and the right ordinate is e_v. This figure indicates that when F_h exceeds 19 $Pa^{0.5}$, e_v rises rapidly corresponding to the surge of h_t (see the dashed line in Figure 9).

In fact, entrainment makes a great contribution to tray efficiency by improving the phase interface. However, it can also cause significant recycle of liquid with large entrainment and the reduction of tray efficiency. The two effects contradict each other and have different effects on efficiency at different flow rates. Figure 10 compares the entrainment curve and the

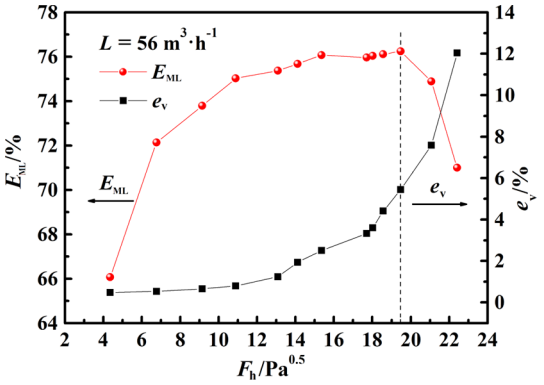

Figure 10. Comparison between entrainment and tray efficiency of the MD sieve tray.

tray efficiency curve of MD sieve tray at 56 m^3 h^{-1}, where the left ordinate is E_{ML} and the right one is e_v. It shows that the phase interface increases with increased gas velocity and the efficiency rises significantly at low gas velocity, where the negative effect of liquid recycle can be neglected due to low entrainment. Afterward, when F_h continues to go up, the increase of efficiency gradually slows, because of the liquid recycle. When F_h approaches 19.3 $Pa^{0.5}$, the efficiency curve declines sharply. It demonstrates that the liquid recycle greatly decreases the driving force for mass transfer while the increased phase interface makes little contribution to efficiency during this stage. Furthermore, the upper limit of the MD tray (6%) is lower than that of the conventional one (10%), because the e_v value of the MD sieve tray is much lower than that of the conventional one.

4. ENTRAINMENT MODEL

4.1. Model Discrimination. In 1955, Hunt et al.[25] gave the empirical entrainment correlation for the conventional sieve tray. This correlation took the disengaging space, T_s-h_{fe}, into account and is applicable for the froth regime.[25,27]

In 1981, Kister et al.[21] founded the entrainment correlation in the spray regime for sieve tray by dimensional analysis, where h_{cl} and physical properties were introduced. In 1982, Fell et al.[27] modified the correlation so that it can be used for different regimes. Then, Kister et al.[22] revised the correlation on the basis of the characteristics of the froth regime. The correction agrees well with the experimental data, which also has good performance on the prediction of nonair/water systems.

In 1995, Bennett et al.[26] discovered another correlation, where e_v is a function of the ratio of tray spacing to froth height (T_s/h_{fe}) and the effective froth density (φ_e). Besides, the expressions of the clear liquid height, the froth height, and the gas holdup are also involved, which make the equations somewhat complicated.

According to the correlation of Fell's correlation,[27] the main parameters, such as u_s, L, φ, d_h, T_s-h_{fe}, are almost taken into account, and it can be extrapolated to other systems, so we regard it as the basic formula for the new model. However, Fell's correlation[27] only applies to the spray- and mixed-froth regime, so we employed it for the mixed-froth regime. On the

DOI: 10.1021/acs.iecr.7b00702
Ind. Eng. Chem. Res. 2017, 56, 6755−6763

other hand, Hunt's correlation[25] is particularly fit for the froth regime, as mentioned previously. Accordingly, we made a derivation in detail on droplets entrained in the froth regime, and got the new formula by using Hunt's correlation[25] for reference.

4.2. Foundation of the New Model. *4.2.1. Mixed-Froth Regime.* The new model of the MD sieve tray in the mixed-froth regime is developed as follows.

$$e_v\ (\%) = K_1\left(\frac{u_s^{K_2}}{L_w^{K_3}}\right)\left(\frac{1}{1+2.62h_w}\right)^{4.68}\left(\frac{h_{cl}}{(d_hT_s)^{0.5}}\right)^{K_4}\left(\frac{\mu_G}{\sigma}\right)^{1.17}\times 100 \tag{2}$$

where h_{cl} can be calculated by the correlations determined in the previous study of this work.[1]

Considering that the only variables investigated in this experiment are u_s, L_w, and h_{cl}, the coefficients of structural and physical property variables are the same as those in the corresponding base models. The new model parameters, K_1–K_4, were acquired by multivariate nonlinear regression of the experimental data in the mixed-froth regime (see Table 3).

Table 3. Entrainment Model Parameters on the MD Sieve Tray: Mixed-Froth Regime

model parameter	regression result
K_1	88.93
K_2	2.779
K_3	0.05152
K_4	0.1474

4.2.2. Froth Regime. The following assumptions are made in the froth regime:

(1) All of the droplets formed on the tray are spherical with a diameter of $[0, d_{max}]$, and the distribution density of droplet diameter, $\varphi(d)$, is a constant in this regime.[32]
(2) The rising droplets are not accelerated, and the relative gas velocity between the droplets and gas is based on the cross-sectional area.
(3) In the froth regime, the maximum diameter of a stable droplet can be determined by Stichlmair's theory of stable large droplets.[33]

Based on assumption (1), we can get

$$\varphi(d) = d\left(\frac{L_s(d)}{L_s}\right) = \text{constant} \tag{3}$$

$F(d)$ is a function that takes values based on a probability distribution; it gives

$$F(d) = \frac{L_s(d)}{L_s} = \frac{d}{d_{max}} \tag{4}$$

where $L_s(d)$ is the volume flow rate of the entrained liquid, L_s is the volume flow rate of the total liquid on the tray, and d_{max} is the maximum diameter of the total stable droplets.

If d_t is the maximum diameter of the droplets entrained to the upper tray, then

$$L_s(d_t) = L_s\left(\frac{d_t}{d_{max}}\right) \tag{5}$$

According to Stichlmair's theory of stable large droplets,[33] it gives

$$W_b = \frac{u_h^{\,2}\rho_G d_{max}}{\sigma} = 12 \tag{6}$$

Then, we can obtain

$$d_{max} = \frac{12\sigma}{u_h^{\,2}\rho_G} \tag{7}$$

According to Steinmeyer's energy dissipation theory, d_t can be rewritten as follows:

$$d_t = k\left[\frac{u_h^{\,2}\rho_G}{g(\rho_L-\rho_G)}\right] \tag{8}$$

and L_s can be expressed by

$$L_s = h_{cl}A_b \tag{9}$$

where A_b is the tray bubbling area.

Substituting eqs 7–9 into eq 5 then gives

$$L_s(d_t) = kh_{cl}A_b\frac{(u_h\sqrt{\rho_G})^4}{12\sigma g(\rho_L-\rho_G)} = kh_{cl}A_b\frac{F_h^{\,4}}{12\sigma g(\rho_L-\rho_G)} \tag{10}$$

The entrainment definition is usually expressed as

$$e_v\ (\%) = \frac{L'}{V'}\times 100 \tag{11}$$

The gas volume (V') is related to T_s–h_{fe}, where h_{fe} is replaced by K_3h_{cl}:

$$h_{fe} = \frac{h_{cl}}{\phi_e} = K_3h_{cl}$$

Therefore, the basic form of the e_v correlation in the froth regime can be derived as eq 12.

$$e_v\ (\%) = \frac{L_s(d_t)\rho_L}{(T_s-K_3h_{cl})A_b\rho_G} = Kh_{cl}\left(\frac{\rho_L}{\rho_G}\right)\left(\frac{1}{\rho_L-\rho_G}\right)\left(\frac{1}{g\sigma}\right)\left(\frac{F_h^{\,4}}{T_s-K_3h_{cl}}\right)\times 100 \tag{12}$$

On the basis of Hunt's correlation, eq 12 can be rewritten as follows:

$$e_v\ (\%) = K_1h_{cl}^{K_2}\left(\frac{\rho_L}{\rho_G}\right)\left(\frac{1}{\rho_L-\rho_G}\right)\left(\frac{1}{g\sigma}\right)\left(\frac{u_s}{T_s-K_3h_{cl}}\right)^{K_4}\times 100 \tag{13}$$

The new model parameters, K_1–K_4, were acquired by multivariate nonlinear regression of the experimental data in the froth regime (see Table 4).

4.2.3. Error Analysis. The correlation coefficient of new model is 0.984 in the mixed-froth regime and 0.992 in the froth

Table 4. Entrainment Model Parameters on the MD Sieve Tray: Froth Regime

parameter	regression result
K_1	2.977×10^{-7}
K_2	−0.7998
K_3	9.264
K_4	7.223

DOI: 10.1021/acs.iecr.7b00702
Ind. Eng. Chem. Res. 2017, 56, 6755–6763

regime. The comparison between the predicted and experimental values of MD sieve tray on entrainment is shown in Figure 11. The average relative deviation of the new model, compared with the experimental data, is ±8.60%, with a maximum value of ±19.65%.

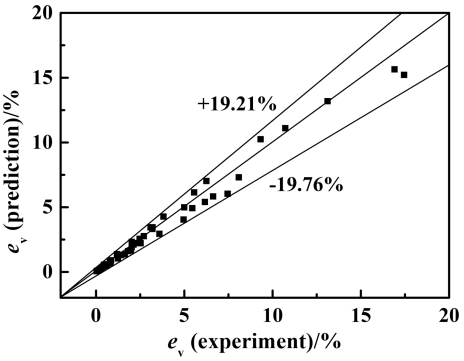

Figure 11. Comparison between predicted data and experimental data of MD sieve tray on entrainment.

It is necessary to determine the operating state on the tray and then select the corresponding formula. Accordingly, we need to establish the criterion for judgment. Considering that h_{cl} is more stable than L_w and the expression, $h_{cl,t}/d_h$, with no dimension, is easy to extrapolate, $h_{cl,t}/d_h$ is employed as the criterion. The critical points (see points a−e in Figure 12) are

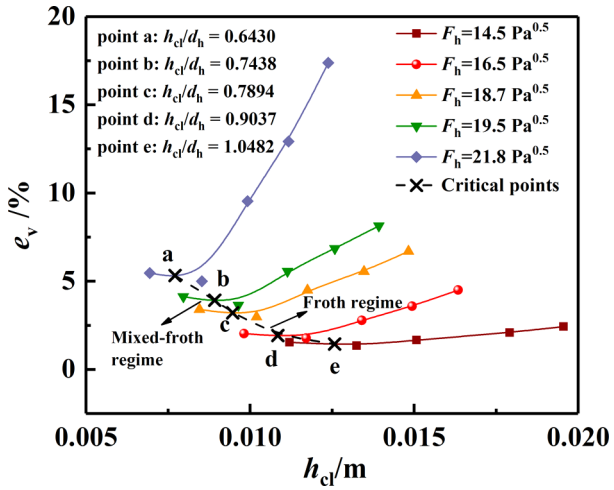

Figure 12. Transition criterion of flow regimes for the MD sieve tray.

obtained from the h_{cl} experimental data. Consequently, the operating range can be divided into two regions by these critical points, that is, the region on the left of the dashed curve is in the mixed-froth regime, while the region on the right of the dashed curve is in the froth regime.

4.3. Validation. *4.3.1. Comparison between the New Model and Kister and Fell's Correlation.* Figure 13 compares the new entrainment correlations (eqs 2 and 13) with the correlations of Fell.[27] They are both evaluated by the experimental data of the MD tray in this work. Note that the calculated data of the correlation of Fell[27] are much higher than the experimental data; however, the new correlation is in accordance with the experimental data. As a result, the applicability of the new correlation for MD trays was verified.

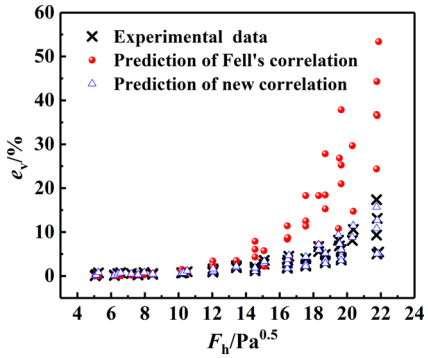

Figure 13. Comparison between predicted data and experimental data of e_v on the MD sieve tray.

4.3.2. Industrial Validation of Pressure Drop. The experimental data of pressure drop obtained in this work has been validated by the industrial data of the ethylene stripping tower (MD sieve) in the gas fractionation unit of Beijing Yanshan Petrochemical Company (SINOPEC).[1] Table 5 compares the experimental and the industrial pressure drop data, where the relative deviation is 6.15%. It indicates the high accuracy of the experimental data of pressure drop. Although the entrainment data in industry cannot be obtained, the consistency of the entrainment- and pressure drop data confirms the reliability of the experimental entrainment data, to some extent.

5. CONCLUSIONS

The following conclusions have been reached in this paper:

(1) The entrainment data were obtained in the experiment of this work. Based on the cited data, the "Double-Transition Point Theory" is concluded to interpret the special entrainment mechanism of the multidowncomer (MD) sieve tray. The MD sieve tray, which usually operates at high liquid load, is mainly in the froth regime or mixed-froth regime when entrainment occurs. This implies a lower entrainment of the MD sieve tray. Moreover, the disengaging space above the dispersion layer is considered as the controlling factor for MD, which makes e_v increase with increased L. It agrees well with the e_v curve on the right side of the second transition point.

(2) The entrainment of the MD sieve tray has a corresponding relationship to the pressure drop of the tray. The pressure drop includes the extra surface energy needed to form droplets, where the higher the pressure drop, the finer and more mist present. In other words, the liquid would be entrained more easily. If the entrainment is excessive, the liquid downstream would be blocked and the pressure drop would surge. The transition points of the two curves coincide with each other.

(3) The entrainment of the MD sieve tray is also closely related to the efficiency. It can be attributed to two aspects from dynamics and thermodynamics. At lower gas velocity, the phase interface is considered to be the controlling factor and can be beneficial to the efficiency from dynamics; while excessive entrainment has a bad effect on the driving force for mass transfer due to liquid recycle, that is, the reduction of the concentration difference causes a heavy loss on efficiency from thermodynamics. The transition points of the e_v curve and E_{ML} curve coincide with each other.

(4) By means of model discrimination, the new MD models was obtained, where Fell's correlation and Hunt's correlation

DOI: 10.1021/acs.iecr.7b00702
Ind. Eng. Chem. Res. 2017, 56, 6755−6763

Table 5. Comparison of the Experimental and Industrial Pressure Drop Data of the Ethylene Stripping Column

structural parameters		process parameter	comparison of pressure drop[a]
tower diameter = 2.6 m	open area = 8.3%	V = 3410 m^3 h^{-1}	$h_{t,overall\ tower,ind}$ = 8.72 kPa
hole diameter = 0.012 m	tray spacing = 0.5 m	L = 28.61 m^3 h^{-1}	$h_{t,ind}$ = 100.19 mm
weir length = 10.0 m	downcomer spacing = 1.0 m	ρ_G = 33.82 kg m^{-3}	$h_{t,exp}$ = 106.30 mm
weir height = 0.05 m	downcomer number = 2	ρ_L = 443.58 kg m^{-3}	Δh_t = 6.16 mm
tray number = 6	total tray number = 20	σ = 4.689 dyn cm^{-1}	err h_t = 6.15%

[a]Note: $h_{t,ind} = \frac{8.72 \times 1000}{20 \times 443.58 \times 9.81} = 100.19$ mm. $\Delta h_t = h_{t,exp} - h_{t,ind}$. err h_t (%) = $(h_{t,exp} - h_{t,ind})/h_{t,ind} \times 100$.

were selected as the basic form of the new correlation for the mixed-froth regime and froth regime, respectively. Particularly, we made a semitheoretical derivation on droplets entrained in the froth regime. In addition, $h_{cl,t}/d_h$ is defined as the criterion for the judgment of gas−liquid contact state. The average relative deviation of the new model is ±8.60%, with a maximum value of ±19.65%.

AUTHOR INFORMATION

Corresponding Authors

*(H.G.) Tel.: 86 10 8232 1366. Fax: 86 10 8232 1210. E-mail: hmguo@cugb.edu.cn.

*(Y.L.) Tel.: 86 10 8973 3288. Fax: 86 10 8973 4159. E-mail: wsuper@cup.edu.cn.

ORCID

Rui Cao: 0000-0002-7365-7615

Present Address

§Currently an associate professor at Chemical Engineering College, China University of Petroleum, Beijing 102249, PRC. E-mail:ctray@cup.edu.cn.

Notes

The authors declare no competing financial interest.

ACKNOWLEDGMENTS

The authors thank the National Natural Science Foundation of China (Nos. 21576287 and 21176248) for financial support.

NOMENCLATURE

A_b = tray bubbling area (m^2)
d = diameter of droplets (m)
d_h = hole diameter (m)
d_{max} = maximum diameter of total stable droplets (m)
d_t = maximum diameter of droplets entrained to upper tray (m)
E_{ML} = Murphree liquid-phase tray efficiency (%)
e_v = liquid entrainment rate (%)
F_h = hole kinetic energy factor ($Pa^{0.5}$)
h_{cl} = clear liquid height (m)
$h_{cl,t}$ = critical value of clear liquid height on tray (m)
h_{fe} = mean height of two-phase dispersion on tray (m)
h_t = tray pressure drop (m)
h_w = weir height (m)
K_1−K_4 = model parameters
L = liquid flow rate (m^3 h^{-1})
L' = entrained liquid mass flow rate (kg s^{-1})
L_w = liquid flow rate per unit weir length (m^3 m^{-1} h^{-1})
L_s = volume flow rate of total liquid on tray (m^3 h^{-1})
T_s = tray spacing (m)
T_s−h_{fe} = disengaging space (m)
u_h = hole gas velocity (m s^{-1})
u_s = superficial gas velocity based on bubbling area (m s^{-1})
V = gas flow rate (m^3 h^{-1})
V' = gas mass flow rate (kg s^{-1})
X_{in} = oxygen concentration of liquid at inlet (mg L^{-1})
X_{out} = oxygen concentration of liquid at outlet (mg L^{-1})
X^*_{out} = equilibrium oxygen concentration of liquid at outlet (mg L^{-1})

Greek Letters

σ = liquid surface tension (N m^{-1})
ρ_G, ρ_L = gas and liquid density (kg m^{-3})
μ_G = gas viscosity (Pa s)
ϕ = fractional hole area (%)
ϕ_e = effective froth density

Subscripts

cl = clear liquid
e = effective
exp = experiment
fe = dispersion layer
G = gas
h = based on hole cross-sectional area
in = inlet
ind = industry
L = liquid
max = maximum
out = outlet
s = based on bubbling area
t = tray
w = weir

REFERENCES

(1) Cao, R.; Liu, Y. S. Pressure Drop Characteristic of Multi-downcomer sieve tray. *Petrol. Refin. Eng.* **2009**, *39*, 36−40.

(2) Delnicki, W. V.; Wagner, J. E. Performance of Multiple Downcomer Trays. *Chem. Eng. Prog.* **1970**, *66*, 50.

(3) Resetarits, M. R.; Miller, R. J. Increase Demethanizer Efficiency and Capacity. *Hydrocarbon Process.* **1991**, *71*, 79−81.

(4) Nutter, D. E. The MVG Tray at FRI. *Chem. Eng. Res. Des.* **1999**, *77*, 493−497.

(5) Yu, X. M.; Xu, C. S.; Zhu, J. Z. Research and Applications of MD Sieve Tray. *Chem. Eng. Des.* **1994**, *6*, 17−20.

(6) Zhao, B. R.; Li, G. H.; Wang, S. H.; Li, S. B.; et al. Brief Summary of the Tianjin Ethylene Plant Revamping by Using Domestic Technology. *Chem. Ind. Eng. Prog.* **2002**, *21*, 626−629.

(7) Zhu, L. Y.; Liu, B. Z.; Lü, Y. J.; et al. Bottleneck Analysis and System Retrofit of Ethylene Splitter. *Petrochem. Technol.* **2003**, *32*, 700−703.

(8) Qi, D. F.; He, J. F.; Yao, K. J. Application of DJ-5 Type Tray in Revamping of C3-splitter in Ethylene Plant in Yanshan. *Mod. Chem. Ind.* **2014**, *34*, 128−130.

(9) Wang, L.; Yang, B. G. Revamping of Raffinate Column in p-Xylene Unit. *Petrol. Refin. Eng.* **2005**, *35*, 22−28.

(10) Yao, K. J.; Zhang, Y. C.; Wang, L. H.; et al. Research and Applications of High Efficiency and High Capacity DJ Series Tray. *Chem. Ind. Eng. Prog.* **2003**, *22*, 228−232.

(11) Yu, X. M.; Zhu, J. Z.; Li, O.; et al. DJ Tray-a Kind of Tray with High Flow Capacity. *Proc. Equip. Des.* **1997**, *34*, 42−45.

DOI: 10.1021/acs.iecr.7b00702
Ind. Eng. Chem. Res. 2017, 56, 6755−6763

(12) Yu, X. M.; Zhu, J. Z.; Xu, C. S. The Present Situation and Prospect of DJ Tray in Industrial Applications. *Chem. Eng. China* **1995**, *23*, 43−46 67.
(13) Chen, X. J.; He, Y. Application of DJ-3 Type Tray on Evaporation Tower in Reforming Unit. *Petrochem. Equip. Technol.* **2005**, *26*, 19−21.
(14) Zhang, Z. Q. Simulation and Efficiency of Multiple Downcomer Tray. *J. Chem. Eng. Chin. Univ.* **1994**, *8*, 250−257.
(15) Fitz, J. C. W.; Kunesh, J. G. Column Hydraulics: System Limit/Ultimate Capacity. *Chem. Eng. J.* **2002**, *88*, 11−19.
(16) Stupin, W. J.; Kister, H. Z. System Limit: the Ultimate Capacity of Fractionators. *Chem. Eng. Res. Des.* **2003**, *81*, 136−146.
(17) Kister, H. Z. *Distillation Troubleshooting*; John Wiley: Hoboken, NJ, 2005; pp 409−410.
(18) Van Sinderen, A. H.; Wijn, E. F.; Zanting, R. W. J. Entrainment and Maximum Vapour Flow Rate of Trays. *Chem. Eng. Res. Des.* **2003**, *81*, 94−107.
(19) Lockett, M. J.; Rahman, M. A.; Dhulesia, H. A. The Effect of Entrainment on Distillation Tray Efficiency. *Chem. Eng. Sci.* **1983**, *38*, 661−672.
(20) Jaćimović, B. M. Entrainment effect on tray efficiency. *Chem. Eng. Sci.* **2000**, *55*, 3941−3949.
(21) Kister, H. Z.; Pinczewski, W. V.; Fell, C. J. D. Entrainment from Sieve Trays Operating in the Spray Regime. *Ind. Eng. Chem. Process Des. Dev.* **1981**, *20*, 528−532.
(22) Kister, H. Z.; Haas, J. R. Entrainment from Sieve Trays in the Froth Regime. *Ind. Eng. Chem. Res.* **1988**, *27*, 2331−2341.
(23) Kister, H. Z.; Haas, J. R. Predict Entrainment Flooding on Sieve and Valve Trays. *Chem. Eng. Prog.* **1990**, *86*, 63−69.
(24) Lu, Y. H.; Duan, D. S.; Zhao, J. F.; et al. On the Two Phase Contact Regimes and the Phase Inversion Points of the Valve Tray. *J. Chem. Ind. Eng. China* **1983**, *34*, 36−45.
(25) Hunt, C. D.; Hanson, D. N.; Wilke, C. R. Capacity Factors in the Performance of Perforated-plate Columns. *AIChE J.* **1955**, *1*, 441−451.
(26) Bennett, D. L.; Kao, A. S.; Wong, L. W. A Mechanistic Analysis of Sieve Tray Froth Height and Entrainment. *AIChE J.* **1995**, *41*, 2067−2082.
(27) Lockett, M. J. *Distillation Tray Fundamentals*, 2nd Edition; Cambridge University: New York, 1986; pp 94−98.
(28) Uys, E. C.; Schwarz, C. E.; Burger, A. J.; et al. New Froth Behavior Observations and Comparison of Experimental Sieve Tray Entrainment Data with Existing Correlations. *Chem. Eng. Res. Des.* **2012**, *90*, 2072−2085.
(29) Uys, E. C.; Burger, A. J.; Du Preez, L. J.; Knoetze, J. H.; et al. The Influence of Gas Physical Properties on Entrainment inside a Sieve Tray Column. *Chem. Eng. Res. Des.* **2015**, *104*, 429−439.
(30) Uys, E. C.; Burger, A. J.; Du Preez, L. J.; Knoetze, J. H.; et al. The Influence of Liquid Physical Properties on Entrainment inside a Sieve Tray Column. *Chem. Eng. Res. Des.* **2017**, *117*, 205−217.
(31) *Technology of Modern Columns*, 2nd Edition; Wang, X. Q., Pan, X. Y., et al., Eds.; China Petrochemical: Beijing, 2005.
(32) Weiss, S.; Longer, J. Mass Transfer on Valve Trays with Modifications of the Structure of Dispersions. *Inst. Chem. Eng. Symp. Ser.* **1979**, *56*, 3.
(33) Stichlmair, J. Maximale Gasbelastung von Kolonnenböden. *VT, Verfahrenstech.* **1974**, *8*, 242−254.

DOI: 10.1021/acs.iecr.7b00702
Ind. Eng. Chem. Res. 2017, 56, 6755−6763